



Cite this: *Dalton Trans.*, 2019, **48**, 5491

Received 15th February 2019,

Accepted 12th March 2019

DOI: 10.1039/c9dt00688e

rsc.li/dalton

## Molecular and electronic structure of the dithiooxalato radical ligand stabilised by rare earth coordination†

Jake McGuire, Bradley Wilson, James McAllister, Haralampos N. Miras,  Claire Wilson,  Stephen Sproules \* and Joy H. Farnaby \*

**Heterometallic rare earth transition metal compounds of dithiooxalate (dto)<sup>2-</sup>, [Ni<sup>II</sup>{(dto)Ln<sup>III</sup>Tp<sub>2</sub>}<sub>2</sub>] (Ln = Y (1), Gd (2); Tp = hydrotris(pyrazol-1-yl)borate) were synthesised. The Lewis acidic rare earth ions are bound to the dioxolene and chemical reduction of 1 and 2 with cobaltocene yielded [CoCp<sub>2</sub>]<sup>+</sup>[Ni<sup>II</sup>{(dto)Ln<sup>III</sup>Tp<sub>2</sub>}<sub>2</sub>]<sup>•-</sup> Ln = Y (3), Gd (4). The reduction is ligand-based and 3 and 4 are the first examples of both molecular and electronic structural characterisation of the dithiooxalato radical (dto)<sup>3•-</sup>.**

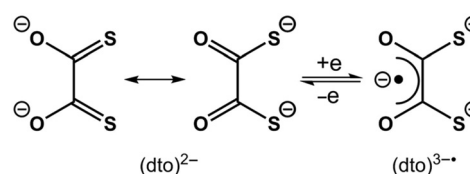
A century of coordination chemistry of the dithiooxalate ligand, (dto)<sup>2-</sup>, has revealed a unique set of properties that sets it apart from other 1,2-dithiolate ligands, *i.e.* dithiolenes.<sup>1,2</sup> The utility of this ditopic ligand stems from the asymmetry of the two binding sites: mid-to-late transition metal ions bind preferentially to the soft sulfur-donor dithiolate, whereas Lewis acidic metal ions bind preferentially to the hard oxygen-donor  $\alpha$ -diketonate.<sup>2</sup> This has led to the assembly of numerous mixed-metal oligomers and coordination polymers by simply combining hard and soft metal ions with a dithiooxalate salt in a one-pot reaction.<sup>3–6</sup> The majority of these studies have focussed on the structural topology of the metal ions, and the magnetic properties of the constituent metal ions linked by this ligand.

The electron transfer chemistry, inherent to bis(dithiolene) compounds, does not exist in monometallic bis(dithiooxalate) species such as [Ni(dto)<sub>2</sub>]<sup>2-</sup>.<sup>2</sup> This stems from the resonance stabilisation within the (dto)<sup>2-</sup> ligand, between the dithiolate and diolate forms (Scheme 1). Prior to this work the only example of reversible one electron transfer chemistry using (dto)<sup>2-</sup> was [M{(dto)SnX<sub>4</sub>}<sub>2</sub>]<sup>2-</sup> (M = Ni, Pd, Pt; X = F, Cl).<sup>5,6</sup> Akin to bis(dithiolene) compounds,<sup>7</sup> the redox chemistry was shown to be ligand-based, with consecutive electrons added to a  $\pi^*$

orbital stabilised by coordination of the Lewis acidic Sn, generating the  $\alpha$ -diketonate radical chelate (dto)<sup>3•-</sup>.<sup>8</sup> However, attempts to isolate and characterise the one electron reduced compounds, were unsuccessful.

Herein we report the synthesis and characterisation of two heterometallic compounds [Ni<sup>II</sup>{(dto)Y<sup>III</sup>Tp<sub>2</sub>}<sub>2</sub>] (1) and [Ni<sup>II</sup>{(dto)Gd<sup>III</sup>Tp<sub>2</sub>}<sub>2</sub>] (2) (Tp = hydrotris(pyrazol-1-yl)borate), in which the  $\alpha$ -diketonate site is occupied by Lewis acidic rare earth ions. Compounds 1 and 2 both display consecutive one-electron reduction waves in their cyclic voltammograms, at reduction potentials that are significantly more negative than [M{(dto)SnX<sub>4</sub>}<sub>2</sub>]<sup>2-</sup>. The chemical reduction of 1 and 2 with cobaltocene yielded [CoCp<sub>2</sub>]<sup>+</sup>[Ni<sup>II</sup>{(dto)Y<sup>III</sup>Tp<sub>2</sub>}<sub>2</sub>]<sup>•-</sup> (3) and [CoCp<sub>2</sub>]<sup>+</sup>[Ni<sup>II</sup>{(dto)Gd<sup>III</sup>Tp<sub>2</sub>}<sub>2</sub>]<sup>•-</sup> (4). The locus of the reduction is confirmed as ligand-based, thus 3 and 4 are the first structurally characterised compounds of the elusive dithiooxalato radical ligand (dto)<sup>3•-</sup>.

Compounds 1 and 2 were synthesised by simultaneous addition of two equivalents of aqueous rare earth chloride and four equivalents of KTp, to a stirred aqueous solution of K<sub>2</sub>[Ni(dto)<sub>2</sub>] at room temperature (Scheme 2). Compounds 1 and 2 precipitated immediately from aqueous solution and were isolated as violet powders in good yields (65–70%). We attribute the increase in yield when compared to related 3d–4f species to the modular approach of using K<sub>2</sub>[Ni(dto)<sub>2</sub>] as a synthon.<sup>4</sup> The simultaneous addition of metal and capping ligand to the reaction mixture limits the formation of [LnTp<sub>2</sub>X] by-products and circumvents the need for several purification



**Scheme 1** Resonance stabilisation and one electron redox chemistry of the (dto)<sup>2-</sup> ligand.

WestCHEM School of Chemistry, University of Glasgow, Glasgow G12 8QQ, UK.

E-mail: stephen.sproules@glasgow.ac.uk, joy.farnaby@glasgow.ac.uk

† Electronic supplementary information (ESI) available: Experimental details, IR spectra, electronic spectra, cyclic voltammogram of 2, crystal structure data, computational data. CCDC 1886429–1886432 and 1889410. For ESI and crystallographic data in CIF or other electronic format see DOI: 10.1039/c9dt00688e



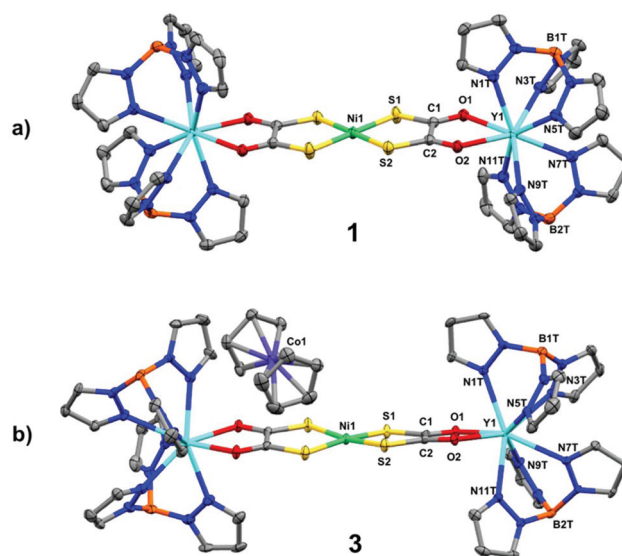
Scheme 2 Synthesis of compounds 1–4.

steps.<sup>9,10</sup> The  $^1\text{H}$  NMR spectrum of **1** in  $\text{C}_6\text{D}_6$  at room temperature displays three resonances at  $\delta = 7.34$ ,  $7.09$ , and  $5.68$  ppm, in the expected 1 : 1 : 1 ratio for magnetically equivalent pyrazolyl rings coordinated to a rare earth ion.<sup>9,11</sup> The BH is observed as a very broad resonance at  $\delta = 4.7$  ppm. We also synthesised  $[\text{PPh}_4]_2[\text{Ni}(\text{dto})\text{SnCl}_4]_2$  **5** to benchmark our experimental data on **1–4**. The ATR IR spectra of **1**, **2** and **5** are consistent with dioxolene binding. The C–O stretching vibrations in **1**, **2** ( $1523$ – $1503 \text{ cm}^{-1}$ ) and **5** ( $1493$ – $1479 \text{ cm}^{-1}$ ) are observed at lower frequency than  $\sim 1600 \text{ cm}^{-1}$  observed in  $[\text{PPh}_4]_2[\text{Ni}(\text{dto})_2]$ .<sup>12</sup>

Based on the first reduction potential of **1** and **2**, determined by electrochemistry (see below), chemical reduction of **1** and **2** with one equivalent of cobaltocene in toluene at room temperature yielded **3** and **4**, respectively (Scheme 2). Compounds **3** and **4** were isolated as teal coloured powders in moderate yields (30–40%). We attribute the successful isolation of the  $(\text{dto})^{3•-}$  radical anion in **3** and **4** to the combined effect of the Lewis acidic rare earth metal and stabilising Tp co-ligands. The purity of **1–5** were confirmed by elemental analysis and all complexes were fully characterised (see ESI† for full experimental details and spectra).

The solid-state molecular structures of compounds **1** and **2** were determined by single crystal X-ray diffraction and are shown in Fig. 1a and Fig. S1.† The square planar  $\text{NiS}_4$  unit has Ni–S bond distances and S–Ni–S angles (Table 1) consistent with those reported for monometallic  $[\text{Ni}(\text{dto})_2]^{2-}$ ,<sup>14</sup> and **5** (Fig. S3†).<sup>6</sup> In **1** and **2** the bridging  $[\text{Ni}(\text{dto})_2]^{2-}$  unit is capped by two eight-coordinate Y or Gd ions whose distorted square antiprismatic geometry is completed by two facially binding Tp ligands. Both complexes are present as *meso* compounds, where one rare earth centre has  $\Lambda$  and the other has  $\Delta$  absolute configuration because of the crystallographic inversion symmetry at Ni.<sup>15</sup> The Ln–O and Ln–N distances fall within the normally observed range. The intraligand S–C, C–C and C–O bond distances (Table 1) do not vary significantly between **1**, **2** and **5**, but do demonstrate the resonance stabilisation (Scheme 1) that gives  $(\text{dto})^{2-}$  its distinctive chemistry in comparison to other 1,2-dithiolenes.<sup>7</sup>

Compounds **3** and **4** are the first examples of structurally characterised dithiooxalato  $(\text{dto})^{3•-}$  ligands in a coordination compound (Fig. 1b and Fig. S2†). Their overall geometry differs from **1** and **2** only by a modest tetrahedralisation of the  $\text{NiS}_4$  core of  $10.3^\circ$  in **3** and  $9.9^\circ$  in **4** (Table 1) and the absence of a crystallographic inversion centre at Ni. The increased charge on the  $(\text{dto})^{3•-}$  ligands significantly shortens the Y–O and Gd–O bonds (Table 1). Reduction of  $(\text{dto})^{2-}$  to  $(\text{dto})^{3•-}$

Fig. 1 Crystal structures of (a) **1** and (b) **3**. Thermal ellipsoids drawn at 50% probability and hydrogen atoms omitted for clarity.Table 1 Selected bond distances and angles<sup>a</sup>

	<b>1</b>	<b>2</b>	<b>3</b>	<b>4</b>	<b>5</b>
M'	Y	Gd	Y	Gd	Sn
Avg. Ni–S	2.1851(9)	2.187(1)	2.168(1)	2.164(1)	2.1803(6)
Avg. M'–O	2.390(2)	2.435(2)	2.326(3)	2.370(3)	2.202(2)
Avg. S–C	1.696(3)	1.699(4)	1.711(4)	1.714(5)	1.681(3)
C1–C2	1.525(5)	1.537(5)	1.468(5) <sup>c</sup>	1.466(5) <sup>c</sup>	1.526(3)
Avg. C–O	1.244(4)	1.241(4)	1.275(5)	1.271(5)	1.248(3)
Avg. M'–N	2.470(3)	2.508(3)	2.497(3)	2.520(4)	
Ni...M'	6.105	6.156	6.071 <sup>c</sup>	6.099 <sup>c</sup>	5.825
M'...M'	12.210	12.313	12.114	12.177	11.650
S–Ni–S	92.78(3)	92.72(4)	92.22(4) <sup>c</sup>	92.21(5) <sup>c</sup>	93.07(2)
O–M'–O	66.23(7)	65.30(8)	68.84(7) <sup>c</sup>	68.0(1) <sup>c</sup>	74.41(6)
$\alpha^b$	0	0	10.3	9.9	0

<sup>a</sup> Distances in angstrom; angles in degrees. <sup>b</sup> Dihedral angle between mean  $\text{NiS}_2$  planes. <sup>c</sup> Average value.

leads to a significant shortening of the C–C bonds and concomitant lengthening of the C–O bonds from those found in **1** and **2** (Table 1). The C–O bond distances in **3** and **4** are consistent with those found in semiquinone ligands<sup>17,18</sup> (quinoidal distortion).<sup>7</sup> This is consistent with the dithiooxalato radical anion  $(\text{dto})^{3•-}$ , with the unpaired electron delocalised over both dto ligands (Fig. 3).



The redox chemistry of **1** and **2** was assessed by cyclic voltammetry (CV) in 5:1 anisole/CH<sub>2</sub>Cl<sub>2</sub> containing 0.2 M [N(<sup>n</sup>Bu)<sub>4</sub>]PF<sub>6</sub> as the supporting electrolyte. Two one-electron processes were evident in voltammograms of both **1** and **2** with reduction potentials of −1.25 and −1.66 V, *versus* the ferrocenium/ferrocene (Fc<sup>+/0</sup>) couple (Fig. 1 inset and S10†). These processes are classed as quasi-reversible, having a large peak-to-peak separation of ~0.2 V. The reduction process is the sequential addition of an electron to each ligand producing (dto)<sup>3•−</sup>, which is stabilised by chelation to the Lewis acidic metal ion. It is important to note that [Ni(dto)<sub>2</sub>]<sup>2−</sup> displays no reversible electrochemistry; rather, there is an irreversible event at −2.49 V that is likely nickel-centred, generating Ni(I), which is unstable in this ligand field.<sup>8</sup> The reduction events of **1** and **2** are consistent with those reported for **5**, but shifted by 0.64 and 0.69 V to more negative potentials, for the first and second reduction respectively.<sup>5,6</sup>

Occupation of the α-diketetonate pocket of the (dto)<sup>2−</sup> ligand is accompanied by a colour change from deep burgundy to violet. In [Ni(dto)<sub>2</sub>]<sup>2−</sup> the transition at 505 nm and shoulder at 564 nm are assigned as metal-to-ligand charge transfer (MLCT) excitations into the π\* orbital of the (dto)<sup>2−</sup> ligand.<sup>13</sup> In heterometallic **1** and **2**, this transition envelope is red-shifted, with two distinct maxima at 592 and 549 nm, and two shoulder features at 620 and 525 nm (Fig. 2 and S5†). A larger red-shift was observed for **5**, with the peaks appearing at 544, 582, 622 and shoulder at 640 nm (Fig. S4†).<sup>6</sup> We attribute this to the higher charge on the Sn(IV) ion and increased covalent character to the bonding in contrast to the rare earth ions in **1** and **2**.

The reduction of **1** and **2** with cobaltocene to yield **3** and **4** was accompanied by a distinct colour change from violet to teal and the appearance of an intense absorption maximum in

the near-infrared (NIR) at 1790 nm ( $\epsilon = 1300 \text{ M}^{-1} \text{ cm}^{-1}$ ) (Fig. 1 and S5†). This is synonymous with bis(dithiolene) transition metal complexes and defined as an intervalence charge transfer (IVCT) transition of the type {Ni<sup>II</sup>(dto<sup>3•−</sup>)(dto<sup>2−</sup>)} ↔ {Ni<sup>II</sup>(dto<sup>2−</sup>)(dto<sup>3•−</sup>)}. This corresponds to a spin-allowed excitation from the highest doubly occupied molecular orbital (HOMO−1) to the singly occupied molecular orbital (SOMO) both of which are ligand-based.<sup>7</sup> This IVCT transition in **3** and **4** is not as intense as seen for bis(dithiolene) complexes, again consistent with an dithiooxalato radical.

The spin ground state of **3** as  $S = 1/2$  was confirmed by EPR spectroscopy (Fig. S11†). The room temperature spectrum revealed a featureless signal at  $g = 2.0033$ . The shift of the  $g$ -value close to that of the free-electron ( $g_e = 2.0023$ ) confirms that the dioxolene of the dto ligand is reduced to produce a dithiooxalato radical. For dithiolene radicals coordinated to Ni(II), the signal is shifted to higher field on account of the spin-orbit contribution from both metal and sulfur atoms.<sup>7</sup> No hyperfine coupling to the <sup>89</sup>Y ( $I = 1/2$ , 100% abundant) nuclei is observed; in contrast to the spectrum recorded on electrochemically-generated [Ni{(dto)SnCl<sub>4</sub>]<sub>2</sub>]<sup>3−</sup>, which exhibited coupling to the spin-active Sn isotopes.<sup>8</sup> However, <sup>89</sup>Y has a significantly smaller nuclear magnetic moment, and the larger spectral linewidth for **3** has obscured any hyperfine structure.<sup>16</sup> Noticeably the frozen solution spectrum recorded at 130 K is near isotropic with  $g = (2.0041, 2.0026, 2.0011)$ , and confirms the spin is almost entirely localised to the dioxolene, with negligible Y content.

The electronic structures of one-electron reduced **1** and **5** have been examined using spin-unrestricted density functional theoretical (DFT) calculations. The Mulliken spin population derived from a single-point calculation on the crystallographic coordinates of **3** revealed the unpaired electron is distributed on the dioxolene of the dto ligand (Fig. 3a). The symmetry of

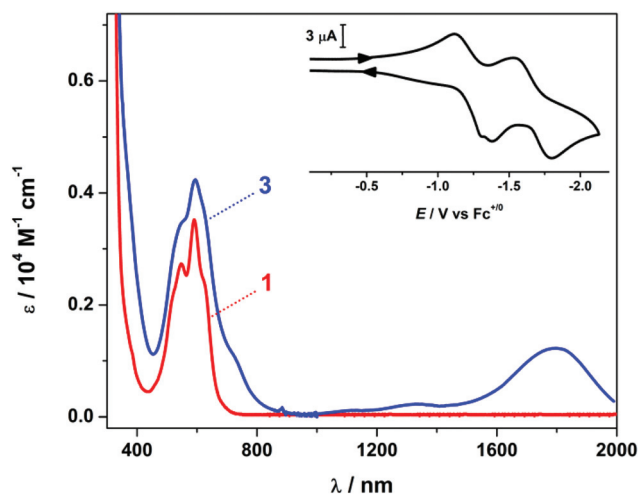


Fig. 2 Overlay of the electronic spectra of **1** and **3** recorded in CH<sub>2</sub>Cl<sub>2</sub> at ambient temperature. Inset shows the cyclic voltammogram recorded in 5:1 anisole/CH<sub>2</sub>Cl<sub>2</sub> containing 0.2 M [N(<sup>n</sup>Bu)<sub>4</sub>]PF<sub>6</sub> at 100 mV s<sup>−1</sup> with potentials referenced to the Fc<sup>+/0</sup> couple.

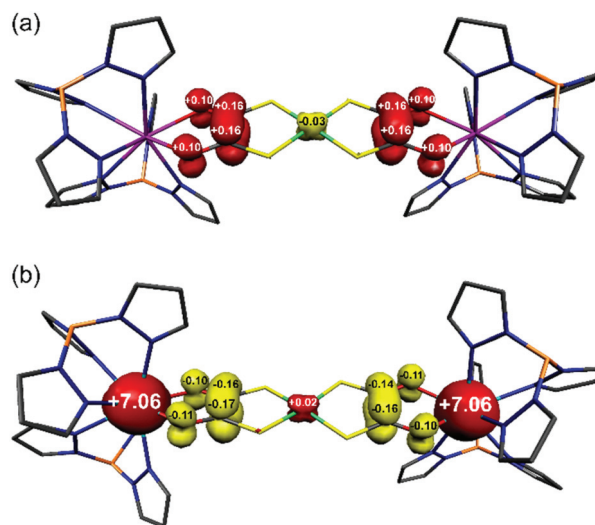


Fig. 3 Mulliken spin population analysis for (a) **3**, and (b) **4** from spin-unrestricted DFT calculations (red: α-spin; yellow: β-spin).





the complex distributes +1.04 spins at each end of the bridging  $\{\text{Ni}(\text{dto})_2\}$  unit with  $-0.03$  spins on the Ni ion from a minor polarisation of the S–C bonds. Notably there is no spin density on the Y(III) ions in accordance with the absence of hyperfine structure in the EPR spectrum. The identical spin distribution is found in the computational one-electron reduced **5**,  $[\text{Ni}\{\text{dto}\text{SnCl}_4\}_2]^{3-}$  (Fig. S14†). As the analogous chemical reduction of **5** was unsuccessful, the electronic structure was calculated on an optimised geometry which exhibited the same intraligand bond distances and angles as seen in **3** and **4** (Fig. S13†).

The electronic structures of **2** and its one-electron reduced product **4** have been calculated using the broken symmetry (BS) method in order to account for the spin coupling between the terminal Gd(III)  $S = 7/2$  ions and  $(\text{dto})^{3*-}$  radical. It has been shown that DFT can reliably estimate the spin coupling between lanthanide ions and organic radicals.<sup>19</sup> A BS(7,7) calculation for **2** gave isoenergetic  $M_S = 0$  state for antiferromagnetically coupled Gd(III) ions, and  $M_S = 7$  for ferromagnetically coupled Gd(III) ions. This implies that two paramagnetic centres are uncoupled, as expected for the 12.31 Å separation with negligible isotropic exchange coupling ( $J \approx 0$ ). Reduction of **2** to **4** introduces a third spin centre into the system, and so BS(14,1), BS(8,7) and BS(7,6) calculations that account for all spin coupled permutations were performed on the crystallographic coordinates of **4** (Table S3†). The results revealed the BS(14,1) solution as the most stable, which is the parallel alignment of the 7 spins on each Gd(III) ions with the opposed alignment of the single spin on the  $(\text{dto})^{3*-}$  ligand, i.e.  $M_S = 13/2$  (Fig. 3b). This solution is marginally more stable than the uncoupled scenario with the Gd(III)-radical exchange interaction estimated at  $J = -1.3 \text{ cm}^{-1}$ . Although small in magnitude, it does fall in the range observed for many other Gd(III)-radical systems.<sup>19</sup> Compound **4** is most closely related to  $[\text{Tp}_2\text{Gd}^{\text{III}}(\text{dtbsq})]$  (dtbsq = 3,5-di-*tert*-butylsemiquinonato), with  $J = -5.7 \text{ cm}^{-1}$ .<sup>17</sup> The smaller exchange interaction estimated for **4** lies in the fact that the  $(\text{dto})^{3*-}$  unpaired electron is delocalised over two dioxolene units in the complex. This reduces the relative spin concentration at each of the four oxygen atoms in  $\{\text{Ni}(\text{dto})_2\}^{*-}$  compared to the two oxygen atoms of *o*-benzosemiquinones.<sup>20</sup> In spite of this, reduction of the bridging  $\{\text{Ni}(\text{dto})_2\}$  unit in **4** enforces a ferromagnetic alignment of the terminal Gd(III) ions, which maximises the total spin ground state of this system, albeit at very low temperatures. This spin distribution in the bridging metallodithiooxalate unit can be modified by changing the metal at its core, which will not only modulate the covalency but also the geometry and therein the alignment of the magnetic anisotropy of the terminal ions, which we will continue to investigate using this system.

In conclusion, heterometallic rare earth transition metal complexes of the  $(\text{dto})^{2-}$  ligand, display ligand-based quasi-reversible electron transfer chemistry. Chemical reduction of these complexes led to the first compounds in which both molecular and electronic structure characterisation of the dithiooxalato radical  $(\text{dto})^{3*-}$  was possible.

## Conflicts of interest

There are no conflicts to declare.

## Acknowledgements

The authors acknowledge the EPSRC (EP/M508056/1 and EP/N509668/1) and the University of Glasgow for funding. The College of Science and Engineering at the University of Glasgow is also acknowledged for a PhD scholarship to BW.

## References

- H. O. Jones and H. S. Tasker, *J. Chem. Soc., Trans.*, 1909, **95**, 1904.
- W. Dietzsch, P. Strauch and E. Hoyer, *Coord. Chem. Rev.*, 1992, **121**, 43.
- (a) P. D. W. Boyd, J. Hope, C. L. Raston and A. H. White, *Aust. J. Chem.*, 1990, **43**, 601; (b) J. M. Bradley, S. G. Carling, D. Visser, P. Day, D. Hautot and G. J. Long, *Inorg. Chem.*, 2003, **42**, 986; (c) D. Coucouvanis and D. Piltingsrud, *J. Am. Chem. Soc.*, 1973, **95**, 5556; (d) M. Leitheiser and D. Coucouvanis, *Inorg. Chem.*, 1977, **16**, 1611; (e) F. J. Hollander and D. Coucouvanis, *Inorg. Chem.*, 1973, **13**, 2381; (f) C. Frasse, J. C. Trombe, A. Gleizes and J. Galy, *C. R. Acad. Sci., Ser. II: Mec., Phys., Chim., Sci. Terre Univers*, 1985, **200**, 403; (g) A. Gleizes, F. Maury, P. Cassoux and J. Galy, *Z. Kristallogr.*, 1981, **155**, 293; (h) J. C. Trombe, A. Gleizes and J. Galy, *C. R. Acad. Sci., Ser. II: Mec., Phys., Chim., Sci. Terre Univers*, 1982, **294**, 1369; (i) A. Gleizes and M. Verdagner, *J. Am. Chem. Soc.*, 1984, **106**, 3727.
- (a) M. Siebold, S. Eidner, A. Kelling, M. U. Kumke, U. Schilde and P. Strauch, *Z. Anorg. Allg. Chem.*, 2006, **632**, 1963; (b) M. Siebold, A. Kelling, U. Schilde and P. Strauch, *Z. Naturforsch., B: J. Chem. Sci.*, 2005, **60**, 1149; (c) M. Siebold, M. Korabik, U. Schilde, J. Mrozinski and P. Strauch, *Chem. Pap.*, 2008, **62**, 487; (d) G.-F. Xu, P. Gamez, J. Tang, R. Clérac, Y.-N. Guo and Y. Guo, *Inorg. Chem.*, 2012, **51**, 5693.
- D. Coucouvanis, *J. Am. Chem. Soc.*, 1970, **92**, 707.
- D. Coucouvanis, N. C. Baenziger and S. M. Johnson, *J. Am. Chem. Soc.*, 1973, **95**, 3875.
- (a) K. Ray, T. Petrenko, K. Wieghardt and F. Neese, *Dalton Trans.*, 2007, 1552; (b) S. Sproules and K. Wieghardt, *Coord. Chem. Rev.*, 2011, **255**, 837.
- G. A. Bowmaker, P. D. W. Boyd and G. K. Campbell, *Inorg. Chem.*, 1982, **21**, 3565.
- T. Sanada, T. Suzuki and S. Kaizaki, *J. Chem. Soc., Dalton Trans.*, 1998, 959.
- T. Sanada, T. Suzuki, T. Yoshida and S. Kaizaki, *Inorg. Chem.*, 1998, **37**, 4712.
- D. P. Long, A. Chandrasekaran, R. O. Day and P. A. Bianconi, *Inorg. Chem.*, 2000, **39**, 4476.



- 12 F. Junnosuke and N. Kazuo, *Bull. Chem. Soc. Jpn.*, 1964, **37**, 528.
- 13 A. R. Latham, V. C. Hascall and H. B. Gray, *Inorg. Chem.*, 1965, **4**, 788.
- 14 P. Román, A. Luque, J. M. Gutiérrez-Zorilla and J. I. Beitia, *Z. Kristallogr.*, 1992, **198**, 213.
- 15 N. G. Connelly, in *Nomenclature of inorganic chemistry. IUPAC recommendations 2005*, Royal Society of Chemistry, 2005.
- 16 (a) D. R. Eaton, *Inorg. Chem.*, 1964, **3**, 1268; (b) B. S. Prabhananda, C. C. Felix, B. Kalyanaraman and R. C. Sealy, *J. Magn. Reson.*, 1988, **76**, 264.
- 17 A. Caneschi, A. Dei, D. Gatteschi, L. Sorace and K. Vostrikova, *Angew. Chem., Int. Ed.*, 2000, **39**, 246.
- 18 (a) A. Caneschi, A. Dei, D. Gatteschi, S. Poussereau and L. Sorace, *Dalton Trans.*, 2004, 1048; (b) J. R. Hickson, S. J. Horsewill, J. McGuire, C. Wilson, S. Sproules and J. H. Farnaby, *Chem. Commun.*, 2018, **54**, 11284; (c) G. H. Spikes, S. Sproules, E. Bill, T. Weyhermüller and K. Wieghardt, *Inorg. Chem.*, 2008, **48**, 10935.
- 19 (a) T. Gupta, T. Rajeshkumar and G. Rajaraman, *Phys. Chem. Chem. Phys.*, 2014, **16**, 14568; (b) T. Rajeshkumar and G. Rajaraman, *Chem. Commun.*, 2012, **48**, 7856.
- 20 R. R. Kapre, E. Bothe, T. Weyhermüller, S. DeBeer George, N. Muresan and K. Wieghardt, *Inorg. Chem.*, 2007, **46**, 7827.

